Virus Research 261 (2019) 31–36

Contents lists available at ScienceDirect

Virus Research

journal homepage: www.elsevier.com/locate/virusres

Naturally-occurring right terminal hairpin mutations in three genotypes of canine parvovirus (CPV-2a, CPV-2b and CPV-2c) have no effect on their growth characteristics

Yongle Yu[a], Jianlou Zhang[b], Jigui Wang[a], Ji Xi[a], Xiaomei Zhang[a], Peiran Li[a], Ying Liu[a], Weiquan Liu[a,*]

[a] State Key Laboratory of Agrobiotechnology, Department of Biochemistry and Molecular Biology, College of Biological Sciences, China Agricultural University, Beijing 100193, PR China
[b] Department of Basic Veterinary Medicine, College of Veterinary Medicine, Agricultural University of Hebei, Baoding, Hebei, 071001, PR China

ARTICLE INFO

Keywords:
Canine parvovirus
Inverted terminal repeats
Mutation
Growth characteristics

ABSTRACT

We have isolated 4 naturally-occurring strains of CPV in mainland China and have identified them as CPV-2, 2a, 2b and 2c genotypes according to their VP2 sequences which also revealed substitutions within their right terminal regions. To determine if these substitutions affected the growth characteristics of the 4 strains, we constructed plasmids based on their genomic sequences minus their right terminal sequences, with the latter replaced by a single right terminal region. Analysis of rescued recombinants showed that the substitutions within their natural right termini had no significant effect on their growth characteristics.

1. Introduction

As an autonomous parvovirus within the family *Parvoviridae*, canine parvovirus 2 (CPV-2) is a nonenveloped icosahedral virus with an single-stranded DNA (ssDNA) genome enclosed within a capsid of diameter ~18-26 nm. Canine parvoviral enteritis, caused by CPV, is an acute infectious disease threatening the dog industry worldwide (Decaro and Buonavoglia, 2012). It is characterized by an acute hemorrhagic diarrhea and rapid reduction in white blood cells, particularly in young animals.

CPV-2 is a virus with a linear negative ssDNA genome of 5.2 kilobases (kb) that encodes four proteins: two nonstructural (NS1, NS2) and two structural (VP1, VP2) (Reed et al., 1988). The coding region of the CPV genome is flanked by inverted terminal repeats (ITRs) in Y- (left end) and U-shaped (right end) configurations, the former of which serves as the origin of replication and contains cis-acting elements and packaging signals (Horiuchi and Shinagawa, 1993; Parrish, 1991). CPV-2 has undergone a rapid genetic evolution and has generated new genotypes (CPV-2a, CPV-2b and CPV-2c) with an amino acid substitution at a position 426 in VP2 (Buonavoglia et al., 2001; Hoelzer and Parrish, 2010). These new types differ from the original CPV-2 by their extended host range, including domestic cats and other nondomestic species (Allison et al., 2013; Battilani et al., 2013).

In China, hemorrhagic enteritis in dogs caused by CPV-2 was first reported in 1983. CPV-2a viruses are distributed all over China, whereas CPV-2b circulates in the south (Zhang et al., 2010; Zhao et al., 2013). CPV-2c was first identified in Jilin province with two reports so far in China (Wang et al., 2016). Recently, co-circulation of new CPV-2a and new CPV-2bs has replaced the original CPV-2a and CPV-2bs, becoming the dominant CPV types in China (Geng et al., 2015).

While the eclipse phase of the canine parvoviral replicative cycle has been intensively studied, some crucial steps are still poorly understood, including virion traffic, virion assembly, and viral genome encapsidation. Since the construction of the first infectious clone of canine parvovirus, most previous reports have been focused on structural or nonstructural proteins and little is known about the central roles in replication, the sizes, sequences, and predicted structures of the hairpins at the two ends of its DNA. The viral telomeres of the minute virus of mice (MVM) contain most of the cis-acting information, such as parvovirus initiation factor (PIF)-binding sites (ACGT motif) and the NS1-binding and nick sites (5′-CTWWTCA-3′), required for nicking and covalent attachment of NS1, both of which are required for DNA replication, transcription, and encapsidation (Burnett et al., 2006). In a previous study, the orientation and sequence changes within the two “ears” of the MVM left-end hairpin had minimal effect on viral viability and no influence on packaging strand specificity; however, MVM genomes with single-ear hairpins have been found unable to initiate nonstructural gene expression (Li et al., 2012, 2013).

* Corresponding author.
E-mail address: weiquan8@cau.edu.cn (W. Liu).

https://doi.org/10.1016/j.virusres.2018.12.007
Received 30 October 2018; Received in revised form 11 December 2018; Accepted 13 December 2018
Available online 14 December 2018
0168-1702/

Table 1
Canine parvovirus isolates obtained from field outbreaks in the mainland China.

Virus isolate	Origin	Year	Genotype	GenBank accession number
CPV-L	Beijing	2014	2	MG763189
CPV-BJL1	Shandong	2015	2a	MH106698
CPV-BJL2	Beijing	2015	2b	MH106699
CPV-BJL3	Guangxi	2016	2c	MH106700

Table 2
Primers used for the amplification of the palindromic terminus sequences.

Primers		Product (bp)	Position (nt)[a]
Y-1-F	ATTCTTTAGAACCAACTGACCAA	56	1–56
Y-1-R	CAGCGCGCGTCATCACGTCAT		
Y-2-F	GCTGCGCGCGCTGCCTAC	262	53–314
Y-2-R	ATTTACTCCCTCCATAACTTCCTC		
U-1-F	TGAAAAATCTCAACTAGCACCT	481	4502–4982
U-1-R	CATAGCGGTCTGGTTGATTAAGC		
U-2-F	GCGGTCTGGTTGATTAAGC	94	4982–5075
U-2-R	AAGTATCAATCTGTCTTTAAGGGGG		

[a] Oligonucleotide positions are referred to the genomic sequence of CPV-Y1 strain (GenBank Accession No. D26079).

In the present study, we have applied reverse genetics to show that specific base changes within the right-end hairpin had no effect on viral biological properties compared with wt CPVs. We also show that different CPV antigenic variants can be rescued from infectious plasmids with common palindromic termini sequences.

2. Materials and methods

2.1. Cell culture and viruses

Feline kidney cells (F81 cells), obtained from the American Type Culture Collection (ATCC), were cultured at 37℃ in an atmosphere of 5% CO_2 in Minimum Essential Medium (MEM, Gibco) containing 10% fetal bovine serum (FBS, Gibco).

Four field isolates (CPV-L, CPV-BJL1, CPV-BJL2 and CPV-BJL3) were collected from suspected CPV cases during 2014 and 2016 in different regions of mainland China. A summary of the collection details of samples is presented in Table 1. All isolates were plaque-purified in feline F81 cells and propagated for 10 passages.

2.2. Cloning and analysis of palindromic terminal sequences of CPV

For the palindromic termini, we performed a PCR amplification well established in our laboratory, which has been used to obtain the palindromic termini of mink enteritis parvovirus (MEV) and Aleutian mink disease virus (AMDV) (Mao et al., 2016; Xi et al., 2016). Briefly, the left-end Y-shaped hairpin sequences and right-end U-shaped hairpin sequences were divided into two sections, respectively: Y-1 and Y-2; U1 and U2 (Table 2). PrimeStar GXL DNA polymerase (TaKaRa, Dalian, China) was used to perform PCR with the following cycling conditions: extracted DNA, forward primer Y-1 F (or Y-2 F, U-1 F, U-2 F) (10 mM) 2 μL, dNTP (2.5 mM) 2 μL, 5 × GXL buffer 5 μL, and ddH_2O 12 μL were incubated at 98℃ for 5 min then immediately chilled on ice for 5 min; PrimeStar GXL DNA polymerase was added and incubated at 68℃ for 3 min, followed by 2 μL of reverse primer Y-1R (or Y-2R, U-1R, U-2R) (10 mM). PCR was performed as follows: 98℃ for 5 min; 35 cycles of 98℃ for 10 s, 55℃ for 15 s, 68℃ for 10 s/kb; and 68℃ for 10 min. The purified PCR fragments were cloned into pEASY-Blunt cloning vector (Transgen, Beijing, China) and positive clones were sequenced by the Beijing Genomics Institute (BGI). The secondary structures of both termini were predicted and analyzed using DNAMAN software package (Version 5.2.2, Lynnon Biosoft, Canada).

2.3. Strategies for constructing recombinant plasmids

The infectious virus clones used in this study were derived from CPV infectious virus clone pCPV-BJL1, as previously described (Yu et al., 2017). Briefly, pCPV-L, pCPV-BJL2 and pCPV-BJL3 were constructed based on their own hairpin sequences. For the recombinant plasmids (p'CPV-BJL1, p'CPV-BJL2 and p'CPV-BJL3), the 5′ hairpin region was replaced by the corresponding part of pCPV-L, and the same method was used to generate p'CPV-L. Sequences of all recombinant plasmids were confirmed by sequencing by the Beijing Genomics Institute (BGI).

2.4. Transfection and blind passages

Six-well plastic dishes (Corning, USA) were seeded with F81 cells

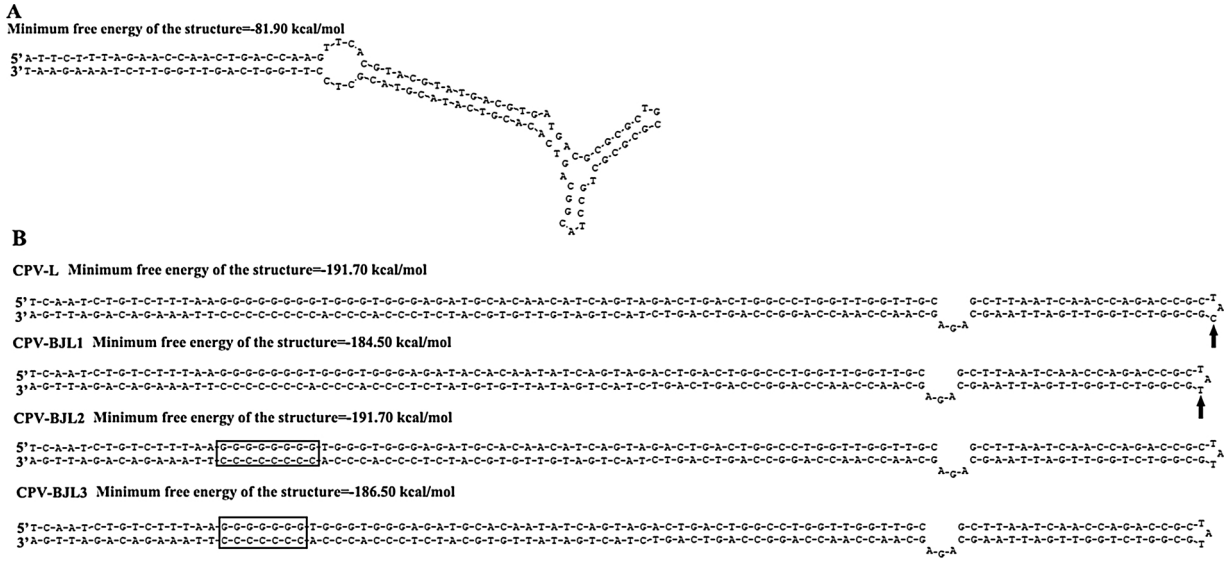

Fig. 1. Sequences and secondary structures of palindromic terminal repeats of CPV isolates. (A) Left-end hairpins of CPV-L, CPV-BJL1, CPV-BJL2 and CPV-BJL3; (B) Right-end hairpins of CPV-L, CPV-BJL1, CPV-BJL2 and CPV-BJL3. Black arrows identify a C–T base mutation in the left-end hairpins of CPV-BJL1, CPV-BJL2 and CPV-BJL3. Black boxed sequences contain a G-C base pair deletion in the right-end hairpins of CPV-BJL1 and CPV-BJL3.

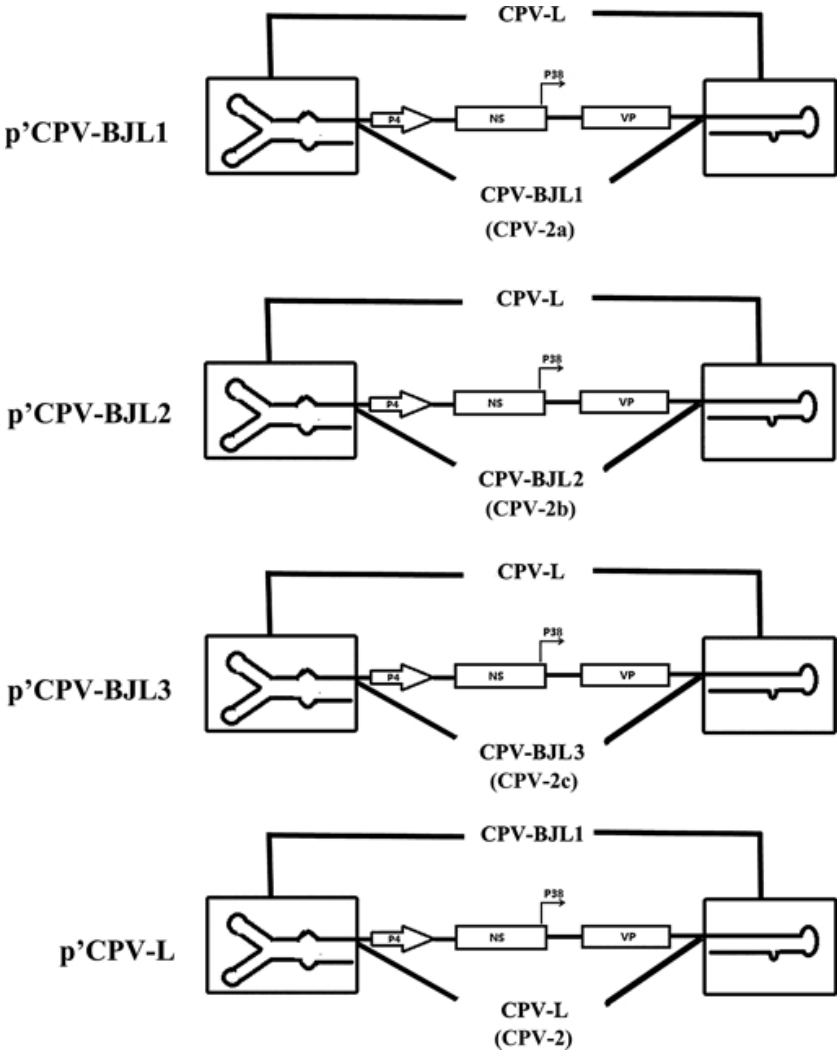

Fig. 2. Diagram of recombinant infectious DNA clones with hairpin regions exchanged. The boxes represent the genomic terminal sequences from CPV-L or CPV-BJL1. The parental viruses: CPV-BJL1, CPV-BJL2, CPV-BJL3 and CPV-L, shown between the boxes, served as the recombinant backbones.

(2×10^5 cells per well) 1 day prior to transfection. Cells at 70%–80% confluence were transfected with purified plasmid DNA (4 μg/well) using Lipofectamine™ 2000 (Invitrogen) according to the manufacturer's instructions. The cultures were maintained in fresh

DMEM/2% FBS (Gibco) for 4 days, following which the cell pellets were collected in 1 ml medium, freeze-thawed 3 times, and the recombinant virus in each lysate was passaged in fresh cell cultures. After 10 passages, viruses were titrated by 50% tissue culture infectious dose ($TCID_{50}$) assay in F81 cells (Sun et al., 2013).

2.5. Virus growth and plaque assay

Multiple-step growth curves were constructed over a 96 h period. F81 cells were seeded in 96-well culture plates at a density of 1×10^4 cells per well in triplicate and allowed to grow for 12 h and then, they were infected with virus at a multiplicity of infection (MOI) of 0.1 and virus titers were monitored at sequential time points by $TCID_{50}$ assay at 4 days post-infection (dpi).

Freeze–thawed virus was diluted to 200 $TCID_{50}$ in 1 ml culture medium and incubated with monolayers of F81 cells for 12 h at 37 °C in 6-well plates. Assays were performed in triplicate for each virus. Supernatants were then removed, and the cells were rinsed 3x with PBS. An overlay medium composed of 2% low melting-point agarose and 2 × DMEM containing 2% FBS was added to the cells. Subsequently, the plate was incubated at 37 °C for 5 days. After plaque formation, cells were fixed with 3.7% formaldehyde and stained with 1% crystal violet.

2.6. Quantitative real-time RT-PCR analysis

F81 cells were incubated with wt or rescued viruses, at an MOI of 2, for 3 h at 37 °C. Cells were gently washed twice to remove unbound virus and incubated with fresh medium for 17 h (total 20 h). Total cellular RNA was extracted and real-time RT-PCR was performed with 1 μg of each RNA sample. First, the RNA was mixed with oligo(dT)18, then denatured at 70 °C for 5 min and transferred immediately to ice. Reverse transcriptase was then added, followed by reaction buffer, dNTP (10 mM) and RNase inhibitor and maintained at 42 °C for 1 h, then 70 °C for 15 min. The cDNA so obtained was used in qPCR with qTOWER-2.2 (Jena, Germany), specific VP2 mRNA primers (forward 5′-GCTTACGCTGCTTATCTTCGC-3′, reverse 5′-TAATGTCCTATTTTCCCC CCC-3′), and real-Time SYBR Master Mix Kit (TaKaRa) according to the manufacturer's instructions. Transcription of mRNA was normalized to β-actin expression (forward 5′-CGGGACCTGACGGACTACCT-3′, reverse 5′-GGCCATCTCCTGCTCAAAAT-3′).

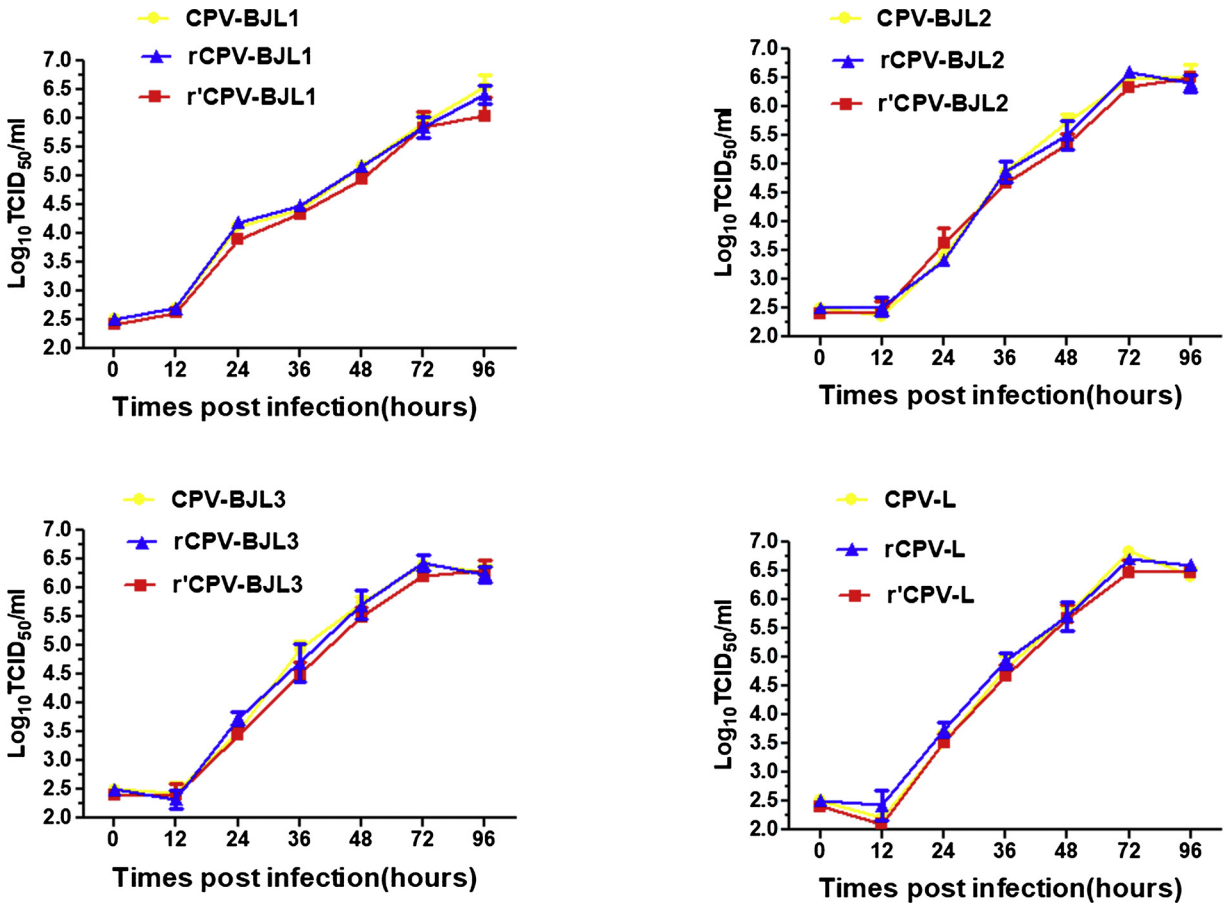

Fig. 3. Growth properties of recombinant viruses in F81 cells. Multistep growth curves of CPV wild-type and recombinant viruses at an MOI of 0.1. Virus titers at different time points, as indicated, were determined by endpoint dilution assay. The error bars indicate standard deviations.

2.7. Indirect immunofluorescence assay

The immunofluorescence assay method has been described previously. F81 cells grown on coverslips were infected with CPV or mock infected. At 48 h postinfection, the cells were fixed with 3.7% paraformaldehyde in PBS and permeabilized with 0.1% Triton X-100 in PBS/2% bovine serum albumin (BSA). After being blocked in PBS/2% BSA for 30 min, the cells were incubated at 37 °C for 1 h with mouse anti-CPV-VP2 monoclonal antibody (Vland Biotech, Qingdao, China) at a dilution of 1:100. The coverslips were washed with PBS 3x for 5 min each time, followed by incubation with fluorescein isothiocyanate (FITC)-conjugated goat anti-mouse IgG Fab' fragment (MBL) at a dilution of 1:100 for 1 h at 37 °C in a humidified chamber. After washing a further 3x with PBS, the cells were observed and photographed using fluorescence microscopy.

2.8. Total protein extraction

F81 cells infected with wt viruses or recombinant viruses (MOI = 1) in 6-well dishes were harvested at 24 h post-infection by removing the medium, washing 3x in cold PBS (pH 7.4), scraping the cells in each well into PBS and centrifuging at 1200 × g for 8 min. Cell pellets were resuspended in 50 µl cold RIPA lysis buffer (50 mM Tris-HCl, pH 7.4, 150 mM NaCl, 1% Nonidet P40, 0.1% SDS) (Huaxingbio) with 0.5 µl 0.1 M PMSF. The lysates were incubated on ice for 30 min and centrifuged at 12,000 × *g* for 30 min at 4℃, then 50 µl supernatants were mixed with 50 µl 2 × SDS sample buffer (100 mM Tris-HCl (pH 6.8), 20% glycerol, 4% SDS, 200 mM dithiothreitol (DTT), 0.1% bromophenol blue) and boiled for 5 min. The protein samples were stored at -70℃ for later analysis.

2.9. Western blot analysis

Following protein extraction, equal amounts of protein samples were resolved by 10% SDS–PAGE and transferred to nitrocellulose membranes (Pall). After blocking with 5% nonfat dried milk in TBST (20 mM Tris-HCl, pH 8.0, 150 mM NaCl, 0.05% Tween-20) for 1 h, membranes were incubated overnight at 4 °C with anti-CPV VP2 mouse monoclonal antibody (diluted 1:1,000, Vland Biotech), anti-CPV NS1 rabbit polyclonal antiserum (diluted 1:5,000) or β-actin mouse monoclonal antibody (diluted 1:1,000, Beyotime) as primary antibodies. After washing with TBST, the membranes were incubated for 1 h with the corresponding horseradish peroxidase HRP]-conjugated anti-rabbit or anti-mouse antibodies (MBL:1:10,000 dilution). All operations were performed at ambient temperature. Target proteins were visualized by enhanced chemiluminescence (ECL) Western blot detection (Thermo). Beta-actin was included as an internal control. Protein bands were quantified by densitometry using Image J software (National Institute of Mental Health, Bethesda, MD, USA).

2.10. Statistical analysis

Data are reported as mean ± SD of three independent experiments, and were analyzed by Student's *t*-test Analyses were performed with GraphPad™ Prism software, version 6.

3. Results

3.1. Comparison of the genome end hairpins of CPV isolates

Prediction of secondary structures of CPV based on the minimal free

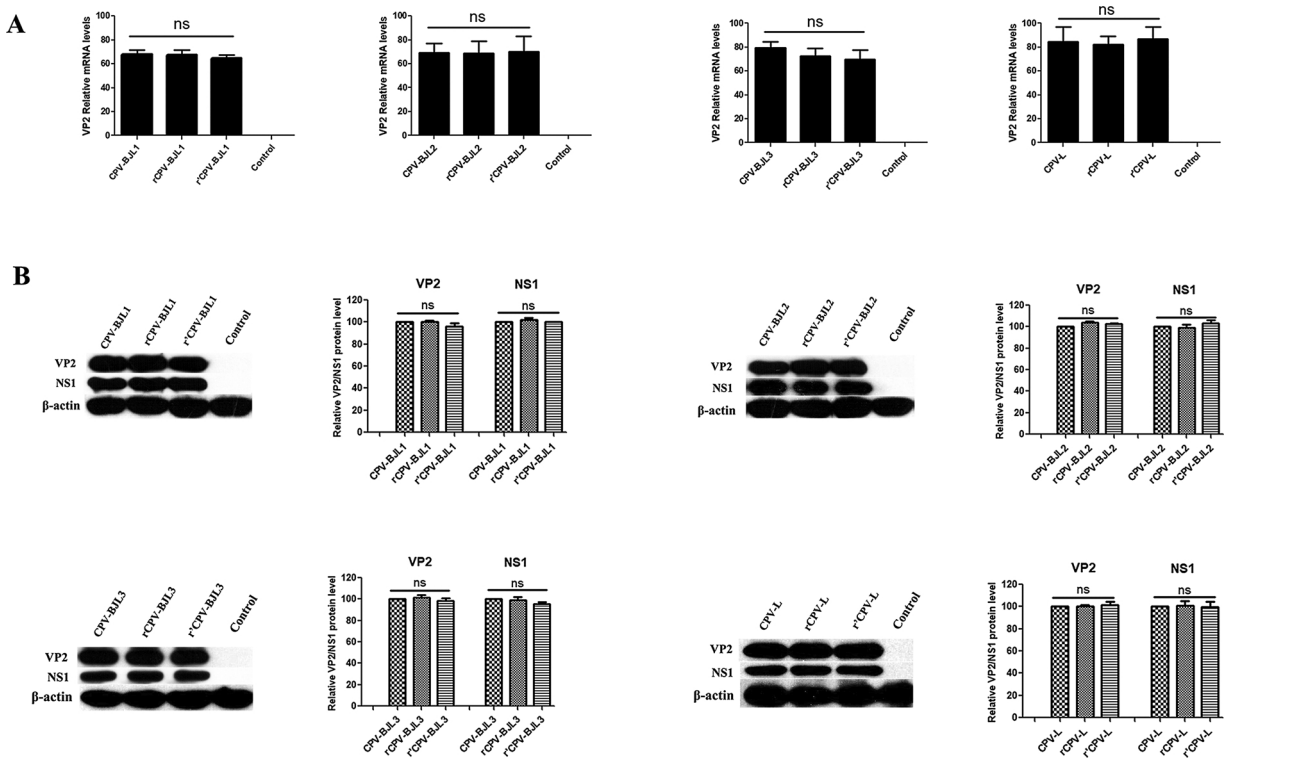

Fig. 4. Comparison of WT or recombinant viruses on viral RNA synthesis and viral translational capacity in F81 cells. (A) Real-time quantitative PCR results showing VP2 mRNA expression. F81 cells were incubated with virus (MOI = 2) for 3 h at 37 °C. Cells were gently washed twice to remove unbound virus and cultured in fresh medium for 17 h (total 20 h). The total RNA was extracted from infected F81 cells at 3 h or 20 h p.i., 1 μg of which was reverse transcribed using oligo-dT18. The mRNA expression levels of the VP2 gene were monitored between 3 h and 20 h p.i. by qPCR with β-actin mRNA levels as a control. (B) Western blot analysis of viral VP2 and NS1 proteins. F81 cells were infected with the parental and recombinant viruses at an MOI of 1 and cell lysates were extracted after 18 h and subjected to Western blot analysis. The membranes were probed with antibodies specific to the CPV VP2 and NS1 proteins.

energy (ΔG) showed that the left-end ITRs were folded into Y-shaped hairpin structures featuring small internal palindromes (26 nt) that together formed the "long ear" (15 nt) and "short ear" (11 nt) of the Y, and a duplex stem region interrupted by a mismatched "bubble" sequence and a asymmetric adenosine residue (Fig. 1A). Based on the minimal free energy (ΔG) of the structure, the right 188 bp (or 186 bp) palindromic terminal sequence of CPV could fold into a U-shaped hairpin (Fig. 1B). Compared with the right ITR of CPV-L, CPV-BJL1 and CPV-BJL3 contained a deletion of a GC base pair, with a substitution of a base (C-T) within the axis of CPV-BJL1, CPV-BJL2 and CPV-BJL3. These results suggest that the 3' terminal of CPV genomes has a high sequence consistency, while mutations and deletions in the 5' terminal hairpin region would affect the overall free energy of the predicted secondary structure, resulting in conformational changes and possible effects on the viral properties.

3.2. Construction and recovery of CPV recombinant viruses

To determine whether base changes within the terminal sequences affects CPV replication, transcription and translation levels during infection, infectious DNA clones were constructed by substituting the hairpin R terminal region of the epidemic virulent strains CPV-BJL1, CPV-BJL2 and CPV-BJL3 for that of avirulent strain CPV-L. The resulting constructs were named p'CPV-BJL1, p'CPV-BJL2, p'CPV-BJL3 and p'CPV-L (Fig. 2). Typical CPV CPE similar to that of the parental viruses was observed 72 h after transfection (Supplemental Fig. S1A). The recombinant viruses, which were subsequently named r'CPV-BJL1, r'CPV-BJL2, r'CPV-BJL3 and r'CPV-L, were verified by sequencing the corresponding exchanged regions, and virus infection was confirmed by immunofluorescence staining of the infected F81 cells with mouse monoclonal antibody (Vland Biotech, Qingdao, China) to the VP2 protein (Supplemental Fig. S1B). This showed that recombinant viruses had been successfully rescued by transfecting cells with the corresponding plasmids and could induce efficient infection in F81 cells.

3.3. Changes in 5'U-shaped hairpin does not impact CPV growth

To investigate if introducing of these mutations affected viral replication in cell culture, the growth characteristics of the wild-type and recombinant viruses were evaluated from their multicycle growth kinetics in F81 cells. Multistep growth curves for the recombinant viruses showed that the replication kinetics of all recombinant viruses (r'CPV-BJL1, r'CPV-BJL2, r'CPV-BJL3 and r'CPV-L) did not differ significantly from those of their corresponding wild-types (Fig. 3). These results indicate that the mutations had negligible influence on the replication of CPV in F81 cells. The same conclusion was reached by plaque assay (Supplemental Fig. S2). To evaluate whether introduction of these mutations modulates transcription, mRNA levels of the VP2 gene were determined by quantitative PCR (qPCR). Results showed that mRNA levels of all the recombinant viruses were no different from the parental strains (Fig. 4A). Western blot analyses based on protein lysates from F81 cells infected with recombinant viruses, showed that VP2 and NS1 expression of the mutants was similar to that of the parental virus (Fig. 4B). These results showed that the mutations had no significant influence on viral protein expression levels.

4. Discussion

Parvoviruses replicate their short (~5-kb) linear single-stranded DNA genomes using a unidirectional strand-displacement strategy called "rolling hairpin" replication, which is an evolutionary adaptation of rolling circle synthesis (Astell et al., 1985; Berns, 1990). This

adaptation is mediated by small imperfect palindromes positioned at each end of the viral genome, which can fold to create hairpin telomeres containing most of the cis-acting information required for viral DNA replication and packaging. Despite these central roles in replication, the sizes, sequences, and predicted structures of the hairpins can vary remarkably between different genera of the *Parvoviridae* and even between the two ends of a single virus (Cotmore and Tattersall, 2014).

In a previous study (Li et al., 2012), reverse genetics were used to explore the roles of left-end structure for minute virus of mice (MVM) by inverting the orientation of the hairpin "ears", creating an anti-parallel organization absent from the wild-type virus, or to introduce multiple transversions conserving the base composition but changing the sequence of the ears. Surprisingly, this study showed that the inverse orientation, and specific sequence changes within the left hairpin ears, had minimal effect on viral viability and no influence on packaging. These observations suggest that it is the entire left terminal structure rather than the specific sequence within that must be conserved.

Only a few studies have been performed on the right-end hairpin of CPV genomes. Parvoviruses have mismatched or unpaired nucleotides in their 5' terminal hairpins which form a small asymmetric bubble and involve NS1-mediated site-specific nicking at an early step (Berns, 1990). Cotmore and coworkers have identified a binding site, ACCAA CCA, for NS1 on each side of the bubble, very close to it (Cotmore et al., 1995). Costello et al. (1995) demonstrated that a virus lacking a bubble was less infectious and replicated less well than the wild-type virus. As with the left ITR, these data indicate that, for efficient replication, the virus requires an intact 5'U shape structure.

Currently, few full-length terminal hairpin sequences of CPV genomes are available in the GenBank database due to the difficulty of obtaining the palindromic termini *via* PCR. Han et al. (2015) sequenced and analyzed the complete palindromic terminus sequences of two CPV field strains, LZ1 and LZ2, which differed from those of CPV-N, CPV-2a (AJ564427) and Laika either in sequence or in the predicted secondary structure, and they concluded that changes in nt such as mutations, deletions or insertions could alter affect the stability of the structure in a way that might affect viral DNA replication.

In the present study, cloning and analysis of the palindromic termini of four field isolates (CPV-L, CPV-BJL1, CPV-BJL2 and CPV-BJL3) revealed that the 3' termini of CPV genomes have a high sequence consistency, while mutations or deletions in the 5' terminal hairpin regions were such that could affect the overall free energy of the predicted secondary structure, resulting in conformational changes and possible effects on the viral properties. Our data, using a reverse genetics technique to evaluate the contribution of the terminal hairpin mutations to canine parvovirus biological activities *in vitro,* show that mutation of the CPV 5' ITR does not disrupt the replication or infectious abilities of the virus. Furthermore, the same effect was observed for levels of viral transcription and translation, thereby indicating that observed natural differences in the isolates had no effect on the viral replication and assembly processes.

Conflict of interest

All authors declare no conflict of interest.

Acknowledgments

This work was supported by National Key Research and Development Program of China (2016YFD0501001).

Appendix A. Supplementary data

Supplementary material related to this article can be found, in the online version, at doi:https://doi.org/10.1016/j.virusres.2018.12.007.

References

Allison, A.B., Kohler, D.J., Fox, K.A., Brown, J.D., Gerhold, R.W., Shearn-Bochsler, V.I., Dubovi, E.J., Parrish, C.R., Holmes, E.C., 2013. Frequent cross-species transmission of parvoviruses among diverse carnivore hosts. J. VIROL. 87 (4), 2342–2347.
Astell, C.R., Chow, M.B., Ward, D.C., 1985. Sequence analysis of the termini of virion and replicative forms of minute virus of mice DNA suggests a modified rolling hairpin model for autonomous parvovirus DNA replication. J. Virol. 54 (1), 171–177.
Battilani, M., Balboni, A., Giunti, M., Prosperi, S., 2013. Co-infection with feline and canine parvovirus in a cat. Veterinaria italiana 49 (1), 127–129.
Berns, K.I., 1990. Parvovirus replication. Microbiol. Rev. 54 (3), 316–329.
Buonavoglia, C., Martella, V., Pratelli, A., Tempesta, M., Cavalli, A., Buonavoglia, D., Bozzo, G., Elia, G., Decaro, N., Carmichael, L., 2001. Evidence for evolution of canine parvovirus type 2 in Italy. J. Gen. Virol. 82 (Pt 12), 3021–3025.
Burnett, E., Cotmore, S.F., Tattersall, P., 2006. Segregation of a single outboard left-end origin is essential for the viability of parvovirus minute virus of mice. J. Virol. 80 (21), 10879–10883.
Costello, E., Sahli, R., Hirt, B., Beard, P., 1995. The mismatched nucleotides in the 5'-terminal hairpin of minute virus of mice are required for efficient viral DNA replication. J. Virol. 69 (12), 7489–7496.
Cotmore, S.F., Tattersall, P., 2014. Parvoviruses: small does not mean simple. Ann. Rev. Virol. 1 (1), 517–537.
Cotmore, S.F., Christensen, J., Nüesch, J.P., Tattersall, P., 1995. The NS1 polypeptide of the murine parvovirus minute virus of mice binds to DNA sequences containing the motif [ACCA]2-3. J. VIROL. 69 (3), 1652–1660.
Decaro, N., Buonavoglia, C., 2012. Canine parvovirus–a review of epidemiological and diagnostic aspects, with emphasis on type 2c. Vet. Microbiol. 155 (1), 1–12.
Geng, Y., Guo, D., Li, C., Wang, E., Wei, S., Wang, Z., Yao, S., Zhao, X., Su, M., Wang, X., Wang, J., Wu, R., Feng, L., Sun, D., 2015. Co-circulation of the rare CPV-2c with unique Gln370Arg substitution, new CPV-2b with unique Thr440Ala substitution, andnew CPV-2a with high prevalence and variation in heilongjiang province, northeast China. PloS one 10 (9), e0137288.
Han, S.C., Guo, H.C., Sun, S.Q., Shu, L., Wei, Y.Q., Sun, D.H., Cao, S.Z., Peng, G.N., Liu, X.T., 2015. Full-length genomic characterizations of two canine parvoviruses prevalent in Northwest China. Arch. Microbiol. 197 (4), 621–626.
Hoelzer, K., Parrish, C.R., 2010. The emergence of parvoviruses of carnivores. Vet. Res. 41 (6), 39.
Horiuchi, M., Shinagawa, M., 1993. Construction of an infectious DNA clone of the Y1 strain of canine parvovirus and characterization of the virus derived from the clone. Arch. Virol. 130 (3-4), 227–236.
Li, L., Cotmore, S.F., Tattersall, P., 2012. Maintenance of the flip sequence orientation of the ears in the parvoviral left-end hairpin is a nonessential consequence of the critical asymmetry in the hairpin stem. J. Virol. 86 (22), 12187–12197.
Li, L., Cotmore, S.F., Tattersall, P., 2013. Parvoviral left-end hairpin ears are essential during infection for establishing a functional intranuclear transcription template and for efficient progeny genome encapsidation. J. Virol. 87 (19), 10501–10514.
Mao, Y., Wang, J., Hou, Q., Xi, J., Zhang, X., Bian, D., Yu, Y., Wang, X., Liu, W., 2016. Comparison of biological and genomic characteristics between a newly isolated mink enteritis parvovirus MEV-LHV and an attenuated strain MEV-L. Virus genes 52 (3), 388–396.
Parrish, C.R., 1991. Mapping specific functions in the capsid structure of canine parvovirus and feline panleukopenia virus using infectious plasmid clones. Virology 183 (1), 195–205.
Reed, A.P., Jones, E.V., Miller, T.J., 1988. Nucleotide sequence and genome organization of canine parvovirus. J. Virol. 62 (1), 266–276.
Sun, J.Z., Wang, J.G., Yuan, D.L., Wang, S., Li, Z.L., Yi, B., Mao, Y.P., Hou, Q., Liu, W.Q., 2013. Cellular microRNA miR-181b inhibits replication of mink enteritis virus by repression of non-structural protein 1 translation. PloS one 8 (12), e81515.
Wang, J., Lin, P., Zhao, H., Cheng, Y., Jiang, Z., Zhu, H., Wu, H., Cheng, S., 2016. Continuing evolution of canine parvovirus in China: isolation of novel variants with an Ala5Gly mutation in the VP2 protein. Infect. Genet. Evol. 38, 73–78.
Xi, J., Wang, J., Yu, Y., Zhang, X., Mao, Y., Hou, Q., Liu, W., 2016. Genetic characterization of the complete genome of an aleutian mink disease virus isolated in north China. Virus genes 52 (4), 463–473.
Yu, Y., Su, J., Wang, J., Xi, J., Mao, Y., Hou, Q., Zhang, X., Liu, W., 2017. A rapid method for establishment of a reverse genetics system for canine parvovirus. Virus genes 53, 876–882.
Zhang, R., Yang, S., Zhang, W., Zhang, T., Xie, Z., Feng, H., Wang, S., Xia, X., 2010. Phylogenetic analysis of the VP2 gene of canine parvoviruses circulating in China. Virus genes 40 (3), 397–402.
Zhao, Y.B., Lin, Y., Zeng, X.J., Lu, C.P., Hou, J.F., 2013. Genotyping and pathobiologic characterization of canine parvovirus circulating in Nanjing, China. Virol. J. 10 (1), 272.